Canadian Science Publishing
NRC Research Press journals | Publishing Services

Canadian Journal of Chemistry
Revue canadienne de chimie

PAMAM dendrimer: a pH controlled nanosponge

Journal:	*Canadian Journal of Chemistry*
Manuscript ID	cjc-2017-0244
Manuscript Type:	Article
Date Submitted by the Author:	20-Apr-2017
Complete List of Authors:	Maiti, Prabal; Indian Institute of Science, Department of Physics
Is the invited manuscript for consideration in a Special Issue?:	Dendimers
Keyword:	PAMAM, simulation

PAMAM dendrimer: a pH controlled nanosponge

Prabal K. Maiti*

Center for Condensed Matter Theory, Department of Physics, Bangalore, India, 560012

Abstract

Using several hundred nanoseconds long fully atomistic molecular dynamics simulation we demonstrate the pH controlled sponge action of PAMAM dendrimer. We show how at varying pH PAMAM dendrimer acts as a wet sponge: at neutral/low pH the dendrimer expands noticeably and the interior of the dendrimer opens up to host several hundreds to thousands of water molecules depending on the generation number. Increasing the pH (going from low pH to high pH for example) leads to the collapse of the dendrimer size and thereby expelling the inner water which mimics the 'sponge' action. As the dendrimer size swells up at neutral/low pH due to the electrostatic repulsion between the primary and tertiary amines which are protonated at this pH, there is dramatic increase in the available solvent accessible surface area (SASA) as well as solvent accessible volume (SAV).

Keywords: PAMAM, dendrimer, molecular volume, solvent accessible surface area, radius of gyration, nanosponge.

* Corresponding author: maiti@physics.iisc.ernet.in

1. Introduction

Dendrimers [1,2] are perfectly branched monodisperse molecules, which have a well-defined structure and molecular weight. The structure and dynamics of dendrimer is a subject of considerable interest due to their versatile application in various fields [1-5] ranging from catalysis, drug delivery[6-8], lubricants to sensors and as nanoscale scaffold for molecular imprinting[9] and molecular electronics. Many of these applications rely on the pH responsive behavior of this polymer. As a function of generation PAMAM dendrimer has an exponentially growing number of primary and tertiary amines which can be protonated or de-protonated depending on the pH of the solvent molecules. Potentiometric tritation studies [10-13] have demonstrated that at very high pH dendrimer is neutral as none of the primary or tertiary amine group is protonated. At physiological pH 7, most of the primary amines are protonated and by pH 4 all of the tertiary amines are also protonated. The pH controlled charging of PAMAM dendrimer helps it's usage as a perfect binder for negatively charged oligonucleotides or double-stranded DNA[14,15] which has application in antisense therapy as well as gene therapy [16-22]. Recent experiments and simulation have proved their efficiency in siRNA complexation[23-27]as well for siRNA delivery [28-30]. Among other important application of PAMAM dendrimer where pH responsive behavior is used are for drug delivery [5,31] and nano-particle formation through metal-ion complexation [32,33]. Dendrimer also find very important applications in HIV inhibition [34,35], fighting bacterial infections [36] and driving and controlling various self-assembly process [37,38]. All the above applications point to the fact that we need to have complete molecular level understanding of the PAMAM dendrimer over entire generation range at varying pH. Starting the early modeling studies by Goddard and co-workers [1,39,40] a number of theoretical and computer simulation studies have been reported on structural properties of model dendrimer under various conditions [36-54]. These studies gave valuable information concerning size and shape of these polymers. However, properties such as solvent accessible surface area and volume, water contents inside the dendrimer, counterion distribution, effective charges which are critical for various application of dendrimers are difficult to get from such simple model. These require detailed molecular level studies involving explicit water and counterions which are computationally very demanding. Earlier we have reported a detailed study of PAMAM dendrimer up to generation 11 in gas phase using fully atomistic molecular dynamics (MD) simulations [41]. Han et. al.[42] also reported various structural properties of PAMAM dendrimer up to G7 in explicit

water. More recently Opitz and Wagner [43] reported a detailed study of PAMAM dendrimer of generations G3-G6 in methanol solution using fully atomistic simulation. We have also reported simulation studies of PTEIM dendrimer in explicit solvent to validate the results from the Small Angle X-ray experiment (SAXS) [44].Again these studies were limited to lower generation dendrimer (up to G6) and small time scale and none of these studies considered effect of solvent pH. Recently Larson and co-workers have reported long time scale MD simulation of G5 PAMAM dendrimer in ethanol/methanol solution [45] and calculated the size of the dendrimer under various solvent conditions but they also didn't consider the effect of solvent pH and didn't consider issues like counterion distribution, solvent accessibility and void size distribution. Effect of solvent pH on the structure of dendrimer was first studied by Welch and Muthukumar [46] using Monte Carlo simulation of model dendrimer within Debye-Hückel approximation. They predicted almost 180% *increase* in dendrimer size as the ionic concentration and pH of the solvent are changed from very high to very low. However, these studies didn't include the effect of explicit counterions which has very important implications as has been shown by later studies. Later Baker and co-workers [47] using fully atomistic model of PAMAM dendrimer including explicit water and counterions showed in agreement with the results of Welch and Muthukumar that indeed there is significant swelling in the size of the dendrimer in changing the pH of the solution from high to low. However, the explicit water and ion studies were limited to only generation 2 (G2) PAMAM dendrimer and higher generation studies approximated the presence of water using an effective dielectric medium. However, this finding was later contradicted by Terao et. al [48] who studied the pH dependence of model dendrimers (up to G7) using Stochastic Molecular dynamics simulation. Using a short spacer length for G7 dendrimer they observe no size change as a function of pH. To investigate the pH dependence issues further we undertook studies of few generations PAMAM dendrimer in explicit water and ions and elucidated the effect of changing pH on the structure of PAMAM dendrimers [49,50]. However, due to computational cost these studies were limited to only G4-G6 and the simulations were of shorter duration (for few hundred ps only) except for G8 PAMAM dendrimer for which we have performed ~20 ns long MD simulation at various pH conditions [50]. More recently Gurtovenko et. al. [51] have reported simulation results using model dendrimer (both charged and uncharged cases) with explicit counterions and showed significant size and conformational change for certain regime of Bjerrum length in agreement with the previous finding. However, this finding was later contradicted by Giupponi et. al [52] who demonstrated that for charged dendrimer in

the presence of explicit counterions due to local charge neutrality electrostatics interactions are always screened very strongly and hence very weak dependence of the size and conformation of the dendrimer as a function of ionic strength. Later we undertook detail study of PAMAM dendrimer in slat solution both at high pH and neutral pH [53,54] and demonstrated strong dependence of the dendrimer size as a function of pH. Later we also developed GAFF and CHARMM compatible FF for PAMAM dendrimer and found similar pH dependent swelling for both the PAMAM and PETIM dendrimer [55,56]. However, due to computational cost none of the above mentioned studies reported the size of the dendrimer at low pH corresponding to the case when both the primary and tertiary amines are protonated. Also a very recent SANS experiment using the recently commissioned Spallation neutron source at Oak Ridge National lab has demonstrated size invariance over broad range of pH change for G4 PAMAM dendrimer in D_2O solution. However, they have observed significant conformational change in going from high to low pH. All these results prompted us to undertake a detailed study of PAMAM dendrimers of various generations in explicit water and ions at varying pH over longer time scale which was not possible earlier due to the limitation in computational resources. A major goal of this paper is to investigate systematically the pH controlled size, shape and accessible solvent area and volume for various generations PAMAM dendrimers. We also give an estimate of the water content in the interior of the dendrimer at various pH as a function of dendrimer generations. Our study demonstrates that PAMAM dendrimer acts as pH controlled nanoscale sponge and complements other class of phosphorus dendrimer which were shown to behave like nanometirc sponge with the addition of THF in the solution [57].

The paper is organized as follows: in section 2 we give details of building of atomic level model of PAMAM dendrimer of various generations, discuss how we take into account the pH effect and give details of simulation methodologies. In section 3 we give results from our long time MD simulations and finally in section 4 we give a brief summary of the main results and conclude.

2. Model building and Simulation details

We have generated the initial 3 dimensional atomistic structures of PAMAM dendrimers using the CCBB Monte Carlo method [41,58]. The details of the CCBB technique can be found in our earlier publication[41,59]. For completeness we give here a short summary of the method. The

continuous configurational biased (CCB) direct Monte Carlo method is based on the independent rotational sampling (IRS). In IRS method, torsions in the polymer chains are sampled using a weighting function based on the Boltzmann factor of the torsion energy E_t. For IRS, the normalized torsion weighting function (TWF), W_{IRS} is defined as

$$W_{IRS}(\phi) = \frac{g_{IRS}(\phi)}{z_{IRS}} \tag{1}$$

where,

$$z_{IRS} = \int_0^{2\pi} g_{IRS}(\phi) d\phi \tag{2}$$

$$g_{IRS}(\phi) = \exp[-\beta E_t(\phi)] \tag{3}$$

However, the possibility of spatial overlaps between nonbonding atoms can not be excluded in IRS and configurations with impossibly high energy will be generated.

In order to remedy this, nonbonding interactions in the vicinity of the growing chain end and within a cutoff sphere of radius R_C are introduced to the TWF calculation. So, the Boltzmann factor for the nonbonding energy inside the cutoff sphere W_{CCB}, is written as

$$W_{CCB}(\phi_i;\phi_1,...,\phi_{i-1}) = \frac{g_{CCB}(\phi_i;\phi_1,...,\phi_{i-1})}{z_{CCB}(\phi_1,...,\phi_{i-1})} \tag{4}$$

where,

$$z_{CCB}(\phi_1,...,\phi_{i-1}) = \int_0^{2\pi} g_{CCB}(\phi_i;\phi_1,...,\phi_{i-1}) d\phi_i \tag{5}$$

$$g_{CCB}(\phi_i;\phi_1,...,\phi_{i-1}) = g_{IRS}(\phi_i) \exp[-\beta \sum_{j,k} \Theta(R_C - r_{jk}) E_{LJ}(r_{jk})] \tag{6}$$

here atom j belongs to the growing chain end group and atom k is one of the atoms in the grown polymer chains. And $\Theta(R)$ is the Heavyside step function, namely $\Theta(R)=0$ when $R<0$ and $\Theta(R)=1$ when $R\geq 0$.

The torsion energy and nonbond energy within the cutoff radius of growing end were calculated before each chain sampling step for a fixed number of grid points equally separated from 0 to 2π. This helps evaluation of W_{IRS}. $P_{IRS}(\phi)$ is defined as the auxiliary distribution and is given by

$$P_{IRS}(\phi) = \int_0^{\phi} W_{IRS}(\phi')\, d\phi' \qquad (7)$$

A random number ξ, uniformly distributed in the interval [0,1), is drawn and the torsion angle is obtained by requiring

$$P_{IRS}(\phi_i) = \int_0^{\phi} W_{CCB}(\phi)\, d\phi \qquad (8)$$

We have applied the CCB technique to generate 3-d atomistic model of PAMAM dendrimers of generations 1-11, supramolecular assemblies of spherical and cylindrical giant liquid crystalline structure synthesized by Percec and coworkers[60] and various other polymers [61,62].

The initial structure generated though CCB scheme were then subjected to Conjugate Gradient optimization to obtain lower energy configurations. We further annealed the minimized structures at very high temperature and cooled down to room temperature. Then 200-400 ps of dynamics were performed at room temperature in the absence of explicit solvent. The final dynamic structure after 200-400 ps runs was protonated at various levels to mimic the pH condition of the solvent. For pH variation we followed the following convention in accordance with the potentiometric titration studies [12] which demonstrated that: at high pH (~12) none of the primary and tertiary amines are protonated, at neutral pH (~7) almost all the primary amines are protonated and at low pH (~4) all the tertiary amines are also protonated. Baker and co-workers [47] have also used similar conventions in their earlier work. Accordingly, the number of atoms as well as the net charge on the dendrimer change in going from high pH to low pH. In Table 1 we give the summary of the structural information of PAMAM dendrimer at various pH. Charges on the dendrimer monomer at various generations at various pH was calculated using the Qeq charge equilibration [63] method. For neutral pH where all the primary amines are protonated, we found that the change of atomic charges is quite localized; and hence we recalculated only their charges on terminal monomers. However, for low pH where both primary and tertiary amines are protonated, the charge was distributed to the

added proton only for the tertiary proton site. Using the LEAP module in AMBER [64], PAMAM dendrimer of various generation at various protonation levels was immersed in a water box using the TIP3P model for water. The box dimensions were chosen in order to ensure a 10Å solvation shell around the dendrimer structure. In addition, for the high and low pH cases, some waters were replaced by Cl^- counter ions to neutralize the positive charge on the protonated primary and tertiary amine sites on the dendrimer structures. This procedure resulted in solvated structures, containing for example 120,750 atoms for high pH, 120,770 atoms for neutral pH and 156,738 atoms for low pH for various protonation levels of G8 dendrimer. MD simulation was performed using the SANDER module and PMEMD of AMBER8 [64]software suite, using the Dreiding force field [65]. The solvated structures were subjected to 1000 steps of steepest descent minimization of potential energy, followed by another 2000 steps of conjugate gradient minimization. During this minimization the dendrimer structure was kept fixed in their starting conformations using a harmonic constraint with a force constant of 500 kcal/mol/Å^2. This allowed the reorganization of the water molecules to eliminate bad contacts with the dendrimer structure. The minimized structure was then subjected to 45 ps of MD, with 2 fs time step. During the dynamics, the system was gradually heated from 0 to 300 K with harmonic constraints on the solute using the SHAKE method. This was followed by 200 ps constant volume – constant temperature (NVT) dynamics with a temperature-coupling constant of 0.5-1.0 ps on the solute. Finally, 10-20 ns NPT unrestrained production dynamics was carried out with a time constant for heat bath coupling of 1 ps. Such long time was required to get the equilibration of the system. The electrostatics interactions were evaluated with the Particle Mesh Ewald [66] (PME) method, using a real space cut off of 9Å.

3. Results

3.1. Size of the dendrimer

Presence of good solvent like water and electrostatics repulsion between the charges at primary/tertiary amine sites make the dendrimer structure swell significantly at various pH compared to the case when no solvent is present. The degree of swelling can be quantified by calculating the size of the dendrimer structure. A quantitative estimate of the dendrimer size is given by the mean-square radius of gyration $<R_g^2>$. For a dendrimer with N atoms the mean-

square radius of gyration is $< R_g^2 >= \frac{1}{M} < [\sum_{i=1}^{N} m_i \left| r_i - R \right|^2] >$, where R is the center-of-mass of the dendrimer, r_i and m_i are the position and mass of the i-th atom; M is the total mass of the dendrimer. Table 2 gives the value of R_g for various generation PAMAM dendrimers at different pH levels. In Figure 1 we have shown the variation of radius of gyration R_g as a function of generation at different pH levels. We see significant size change in going from high pH to neutral pH. But the size remains almost invariant in going from neutral to low pH within the calculation time of our simulation (~10 ns in most cases, occasionally 20 ns long for some generations). Even though there is no significant size change in going from neutral to low pH, there is very large conformational change in the interior of the dendrimer which are evident from other measurement like water contents, void area and volume as discussed below. The size invariance of the dendrimer in going from neutral to low pH contradicts our earlier finding where we have shown size increase in going from neutral to low pH. This might be an artifact of shorter duration of simulation in our earlier work as well as use different force-field for water and ions.

However, this size invariance is in agreement with the recent neutron scattering study on G4 PAMAM dendrimer [67]. To understand our present results we can envisage several possible scenarios. Gurtovenko et. al. [51] using a coarse-grained model of dendrimer showed that the size increase attains a maxima for certain values of Bjerrum length and then remains unchanged and eventually decreases with further increase in the Bjerrum length. The variation of Bjerrum length can be associated with the dielectric constant of the solvent which in turn depends on the ionic strength of the solvent. Our results might indicate that neutral pH may give rise to that optimum Bjerrum length. To probe this further we computed the Debye length for simulation conditions corresponding to the simulation of G4 PAMAM dendrimer. The Debye length at neutral pH (64 Cl- ions in a simulation box of 280 nm^3) is 6.8 Å and low pH (126 Cl- ions in a simulation box of 373 nm^3) is 5.5 Å . So screening length is actually smaller in case of low pH which will give rise to very strong electrostatic screening. Also it might indicate that at low pH due to the larger number counterions (Cl- ions) present in the system there are larger accumulation of counterions in the interior of the dendrimer leading to the charge neutrality which reduce the electrostatic repulsion and hence the degree of swelling. To understand the local charge neutrality further in figure 2 (a) we plot the total charge density (dendrimer monomer plus counterions) for G4 and G7 dendrimer at neutral and low pH. We see a larger regime of charge neutrality at low pH compared to neutral pH.

This is due to the larger number of counterions within the interior of dendrimer at low pH as is evident from figure 2(b). The higher degree of local charge neutrality results in the cancellation of electrostatic repulsion and hence no significant increase in swelling at low pH. It would be interesting to carry out fully atomistic simulation like those presented here by gradual changing of Debye length in the range studied by Welch and Muthukumar and come up with the correct regime where swelling phenomena can occur and beyond which one may expect size invariance. This will require significant computation cost but nevertheless not a distant goal. pH dependent charge states and the degree of counterion condensation also determines the zeta potential of the dendrimer [54] and control its interaction with lipid bilayer membrane [68].

3.2 Water contents

In the previous section we saw that there is significant change in size of the dendrimer in going from bad solvent to good solvent like water. The degree of swelling further increases with the increase in protonation level of the dendrimer at neutral and low pH. Due to this swelling the interior of the dendrimer opens up and become accessible to the solvent. Consequently, we see that large number of water molecules have penetrated throughout the interior of the dendrimer. In Figure 3 (a)-(b) we have plotted the radial monomer density for G4 and G7 PAMAM dendrimer respectively in water at varying pH conditions. The average radial monomer density is computed by counting the number of atoms whose centers of mass are located within the spherical shell of radius r and thickness Δr. For G4 we find that in the presence of solvent (whether neutral or low pH) the monomer density shows a filled core picture with a density maxima at the core and then shows a minimum at around 10 Å away from the core. This indicates a dense core compared to the middle of the dendrimer, which is fairly hollow. Due to this hollowness at the middle regions of the dendrimer, a significant number of waters penetrate to the middle of the dendrimer. The water density profiles shown in figure 3 (a) supports this picture. Similar density profiles are observed up to G6. We should mention here that appearance of the minimum at certain distance from the core is visible only in simulation with explicit water and ions and will not be observed in gas phase simulation as well in as in coarse-grained model simulation. Beyond G6 the density minima at around 10 Å away from the core vanishes as can be seen from figure 3(b) where we have shown the density profile for G7 at various pH. Similar density profile is also observed for G8. For G7 and G8 (these are the maximum generations studied till date in explicit water and ions at various pH)

the dense core regimes continues further outward and there is large regime of constant density zone in the middle of the dendrimer after which density start decreasing. For these generations also there are large numbers of water penetrating inside the core of the dendrimer. We see that at neutral and low pH when primary and tertiary amines are protonated there is significant increase in the density of water near the core region of the dendrimer compared to the high pH case when none of the amines are protonated. The water density profile shown in figure indicates that large pool of water is available in the interior of the dendrimer which can be used for various applications. To see the change in solvent penetration as the size of the dendrimer increase with generation we have shown the density profile for water molecules for various generation dendrimers at neutral pH in figure 4(a). The density profile for the high pH and low pH show similar behavior. The water density gradually increases as we go radially outward from the center-of-mass of the dendrimer and reaches a constant bulk-like value before decreasing again due to finite size effects. A quantitative estimate of the solvent penetration is given by counting the number of waters bound within the interior of the dendrimer. Due to the non-uniformity of the dendrimer surface special care must be taken to identify the bound water, as simple spherical cutoff will overestimate the numbers of waters within the dendrimer. To have an accurate estimate of the number of bound water we have used following criteria: We first calculated the molecular surface area (MSA) for each of the dendrimer atom using a large probe radius (6 Å). With this probe radius the generated surface of the dendrimer becomes almost spherical and smooth. Those atoms with non-zero MSA represent the surface atoms of the dendrimer. Using these surface atoms we identify all the surface waters that are within 4 Å of the surface atoms. Next we identify all the waters close to the inner atoms (with zero MSA) excluding all the previously defined surface waters. The number of bound waters calculated this way is shown in figure 4(b) and has also been given in Table 3. For example for G4 we have 3 water/primary amine group at high pH and 5 water/tertiary amine group at low pH. The water content increases dramatically for G7 PAMAM dendrimer: 6 water/ primary amine group at high pH and 8 water/tertiary amine group at low pH. Note that the number of inner water for G4-G6 PAMAM dendrimer at various pH levels is slightly different from our earlier reported results [49]. This could be due to the use of different water (F3C vs TIP3P) potential used in our simulation. This significant penetration of solvent molecules inside the dendrimer structure is in agreement with the recent SANS studies on poly (benzyl ether) [69] and polycarbosilane dendrimers [70]. Such large water content inside the dendrimer make it a nano-reactor and can help various catalytic

activities within the inner envelope of dendrimer. Earlier we have also shown [49] that these waters can have very different thermodynamics properties compared to the bulk water. Our estimate of number of inner water can also help explain the large number Cu (II) binding by dendrimer in experimental observations [33]. It is also worth mentioning that the amount of water trapped inside dendrimer of various architecture, and their wet/dry weight ratio has also been recently investigated by means of well-tempered metadynamics [71].

3.3 Solvent accessible molecular surface and volume

To demonstrate the pH controlled sponge action we have also computed the solvent accessible surface area (SASA) and solvent excluded volume (SAV) for various generation dendrimers and show how they change as a function of pH change. For the calculation of SASA and solvent accessible volume we have used Analytical volume generalized Born (AVGB) method developed in Goddard group [72]. AVGB is very fast and accurate and has been applied successfully to study solvation effects in biological systems [73] as well estimating SASA in various DNA based nanostructures [74,75]. The SASA is defined as the surface traced by the center of a spherical solvent probe as it rolls around the van der Waals spheres of the solute (in this case dendrimer).

Figures 5(a)–(b) plot $\sqrt{A_{SASA}}$ as a function of probe radius for PAMAM dendrimers for generations 2 to 7 at high pH and neutral pH solvent conditions. The plot for low pH is qualitatively similar to those at high and neutral pH. These plots show that the SASA increases linearly with the probe radius (except for small probe radius). For small probe radius the deviations from the linear behavior is due to the presence of extra surface in the interior of dendrimer. We see that the available internal surface area increases with the increase in dendrimer generation as well as protonation level. The difference between the calculated points and the line in Figure 5 gives an estimate of the available internal surface area. Table 4 gives the SASA and SAV for various generations PAMAM dendrimer at different pH level for a probe radius of 1.4 Å. The internal surface area is also plotted as a function of pH for a probe radius of 1.4 Å in Figure 7(a) for various generations PAMAM dendrimer. For a given generation the available internal surface area increases dramatically in going from bad solvent to the low pH condition. Such dramatic increase in the available inner surface area makes dendrimer behave like a nanometric sponge as more and more water penetrates in the interior of the dendrimer.

We have also calculated the volume associated with the internal cavities by calculating the volume contained inside the SASA, which is called the *solvent accessible volume* (SAV) as a function of probe radius. For a perfect sphere devoid of internal cavities, the volume contained within the sphere's SASA is given by

$$V_{SAV} = \frac{4}{3}\pi(R+p)^3 \quad (5)$$

Figures 6(a)-(b) show $\sqrt[3]{V_{SAV}}$ as a function of probe radius p for different generations PAMAM dendrimer at high pH and low pH. Neutral pH gives similar plots as a function of probe radius for various generations except that we have larger volume available compared to high pH. For larger probe radius $\sqrt[3]{V_{SAV}}$ is linear in p with a slope $\sqrt[3]{4/3\pi}$. The intercept at zero probe radius leads to an estimate of the volume contained inside the dendrimer, including all internal pores and cavities.

The deviation of the SAV from the line in Figures 6(a)-(b) gives a measure of the volume contained in the internal voids and cavities. The available volume for a probe radius of 1.4 Å is plotted for various generation dendrimers at different solvent conditions in figure 7(b). The nanosponge concept is also closely related to the idea of host/guest properties of dendrimers and makes dendrimer suitable for drug delivery [7,76]. Recently, we have analyzed the release pattern behaviour of four ligands (two soluble drugs namely Salicylic acid (Sal), L-Alanine (Ala) and two insoluble drugs namely Phenylbutazone (Pbz), Primidone (Prim)) which were initially encapsulated inside the dendrimer using docking method. Our simulation study provides a microscopic picture of the encapsulation and controlled release of drugs in the case of dendrimer based host-guest systems [77]. This tight correlation between ability to host guests and to incorporate water has also been described by Pavan et. al. using MD simulations and experiments [78].

4. Concluding Remarks/Summary

Let us summarize the main results of this paper. This is the first systematic investigation of the structure of PAMAM dendrimer up to G8 at a full atomistic level including the effect of explicit water and ions at three well defined pH conditions. Our fully atomistic simulations in explicit water

and ions demonstrate that the size of the dendrimer can be tuned by varying the pH of the solution. There is significant change in size of the dendrimer in going from bad solvent to good solvent. The size increases further in changing the pH of the solvent from 10 (corresponding to high pH case) to 7 (corresponding to neutral pH). However, we don't observe significant size variation in going from neutral to low pH and we argued this effect in terms of the local charge neutrality as a consequence of large counterions penetration in the interior of the dendrimer. How the size changes as one gradually increases in the Debye length will be the subject of future study. As the dendrimer swells significantly in going from high to neutral pH a large number of water penetrates in the interior of the dendrimer and affects the conformation and gets reflected in the monomer and water density distribution. At low pH even though there is no change in size, we do observe significant conformational change as can be seen from the monomer density distribution as well as in increase in the number of water present in the interior of dendrimer. With the lowering of solvent pH due to electrostatics repulsion between the charged primary/tertiary amine groups as well as favorable polar interaction with the water molecules, the interior of the dendrimer opens up with internal cavities available inside. Consequently the available internal solvent accessible surface area and volume dramatically increases as a function of pH as well as with increasing generation. For example for G7 in going from high pH to neutral pH there is almost 180% increase in the available SASA and 210% increase in available SAV for a probe radius of 1.4 Å. Availability of such large inner SASA and opening up of the inner channels which goes all the way from the surface to core of the molecules can help facilitate the use of dendrimer as efficient drug delivery materials, complexation with metallic ions.

Acknowledgement

This work is supported by grants from DST, India.

REFERENCES

(1) Tomalia, D. A.; Naylor, A. M.; Goddard, W. A. *Angewandte Chemie-International Edition in English* **1990**, *29*, 138.

(2) Bosman, A. W.; Janssen, H. M.; Meijer, E. W. *Chemical Reviews* **1999**, *99*, 1665.

(3) Ballauff, M.; Likos, C. N. *Angew. Chem.* **2004**, *43*, 2998.

(4) Lee, C. C.; MacKay, J. A.; Frechet, J. M. J.; Szoka, F. C. *Nature Biotechnology* **2005**, *23*, 1517.

(5) Svenson, S.; Tomalia, D. A. *Advanced Drug Delivery Reviews* **2005**, *57*, 2106.

(6) Tekade, R. K.; Kumar, P. V.; Jain, N. K. *Chemical Reviews* **2009**, *109*, 49.

(7) Jain, V.; Maingi, V.; Maiti, P. K.; Bharatam, P. V. *Soft Matter* **2013**, *9*, 6482.

(8) Tian, W. D.; Ma, Y. Q. *Chemical Society Reviews* **2013**, *42*, 705.

(9) Kim, S. H.; Lamm, M. H. *Polymers* **2012**, *4*, 463.

(10) van Duijvenbode, R. C.; Borkovec, M.; Koper, G. J. M. *Polymer* **1998**, *39*, 2657.

(11) Koper, G. J. M.; vanGenderen, M. H. P.; ElissenRoman, C.; Baars, M.; Meijer, E. W.; Borkovec, M. *Journal of the American Chemical Society* **1997**, *119*, 6512.

(12) Cakara, D.; Kleimann, J.; Borkovec, M. *Macromolecules* **2003**, *36*, 4201.

(13) Niu, Y. H.; Sun, L.; Crooks, R. A. *Macromolecules* **2003**, *36*, 5725.

(14) Nandy, B.; Maiti, P. K.; Bunker, A. *Journal of Chemical Theory and Computation* **2012**, *9*, 722.

(15) Nandy, B.; Maiti, P. K. *Journal of Physical Chemistry B* **2011**, *115*, 217.

(16) Yoo, H.; Juliano, R. L. *Nucl. Acids. Res.* **2000**, *28*, 4225.

(17) Bielinska, A.; KukowskaLatallo, J. F.; Johnson, J.; Tomalia, D. A.; Baker, J. R. *Nucleic Acids Research* **1996**, *24*, 2176.

(18) Zinselmeyer, B. H.; Mackay, S. P.; Schatzlein, A. G.; Uchegbu, I. F. *Pharmaceutical Research* **2002**, *19*, 960.

(19) Hollins, A. J.; Benboubetra, M.; Omidi, Y.; Zinselmeyer, B. H.; Schatzlein, A. G.; Uchegbu, I. F.; Akhtar, S. *Pharmaceutical Research* **2004**, *21*, 458.

(20) Kang, H. M.; DeLong, R.; Fisher, M. H.; Juliano, R. L. *Pharmaceutical Research* **2005**, *22*, 2099.

(21) Maiti, P. K.; Bagchi, B. *Nano Letters* **2006**, *6*, 2478.

(22) Lakshminarayanan, A.; Ravi, V. K.; Tatineni, R.; Rajesh, Y. B. R. D.; Maingi, V.; Vasu, K. S.; Madhusudhan, N.; Maiti, P. K.; Sood, A. K.; Das, S.; Jayaraman, N. *Bioconjugate Chemistry* **2013**, *24*, 1612.

(23) Vasumathi, V.; Maiti, P. K. *Macromolecules* **2010**, *43*, 8264.

(24) Nandy, B.; Santosh, M.; Maiti, P. K. *Journal of Biosciences* **2012**, *37*, 457.

(25) Pavan, G. M.; Mintzer, M. A.; Simanek, E. E.; Merkel, O. M.; Kissel, T.; Danani, A. *Biomacromolecules* **2010**, *11*, 721.

(26) Pavan, G. M.; Posocco, P.; Tagliabue, A.; Maly, M.; Malek, A.; Danani, A.; Ragg, E.; Catapano, C. V.; Pricl, S. *Chemistry-a European Journal* **2010**, *16*, 7781.

(27) Pavan, G. M.; Danani, A. *Physical Chemistry Chemical Physics* **2010**, *12*, 13914.

(28) Tsutsumi, T.; Hirayama, F.; Uekama, K.; Arima, H. *Journal of Controlled Release* **2007**, *119*, 349.
(29) Zhou, J. H.; Wu, J. Y.; Hafdi, N.; Behr, J. P.; Erbacher, P.; Peng, L. *Chemical Communications* **2006**, 2362.
(30) Gary, D. J.; Puri, N.; Won, Y. Y. *Journal of Controlled Release* **2007**, *121*, 64.
(31) Boas, U.; Heegaard, P. M. H. *Chemical Society Reviews* **2004**, *33*, 43.
(32) Diallo, M. S.; Balogh, L.; Shafagati, A.; Johnson, J. H.; Goddard, W. A.; Tomalia, D. A. *Environmental Science & Technology* **1999**, *33*, 820.
(33) Diallo, M. S.; Christie, S.; Swaminathan, P.; Balogh, L.; Shi, X.; Um, W.; Papelis, C.; Goddard, W. A.; Johnson, J. J. *Langmuir* **2004**, *20*, 2640.
(34) Nandy, B.; Saurabh, S.; Sahoo, A. K.; Dixit, N. M.; Maiti, P. K. *Nanoscale* **2016**, *7*, 18628.
(35) Nandy, B.; Bindu, D. H.; Dixit, N. M.; Maiti, P. K. *Journal Of Chemical Physics* **2012**, *139*, 024905.
(36) Mandal, T.; Kanchi, S.; Ayappa, K. G.; Maiti, P. K. *Nanoscale* **2016**, *8*, 13045.
(37) Mandal, T.; Kumar, M. V. S.; Maiti, P. K. *Journal Of Physical Chemistry B* **2014**, *118*, 11805.
(38) Mandal, T.; Dasgupta, C.; Maiti, P. K. *Journal Of Physical Chemistry C* **2013**, *117*, 13627.
(39) Naylor, A. M.; Goddard, W. A.; Keiffer, G. E.; Tomalia, D. A. *J. Amer. Chem. Soc.* **1989**, *111*, 2339.
(40) Naylor, A. M.; Goddard, W. A. Application of Simulation and Theory to Biocatalysis and Biomimetics. In *Biocatalysis and Biomimetics, ACS Symposium Series*; Burrington, J. D., Clark, D. S., Eds.; American Chemical Society: Washington, DC, 1989; Vol. 392; pp Chapter 6.
(41) Maiti, P. K.; Cagin, T.; Wang, G. F.; Goddard, W. A. *Macromolecules* **2004**, *37*, 6236.
(42) Han, M.; Chen, P. Q.; Yang, X. Z. *Polymer* **2005**, *46*, 3481.
(43) Opitz, A. W.; Wagner, N. J. *Journal of Polymer Science Part B-Polymer Physics* **2006**, *44*, 3062.
(44) Jana, C.; Jayamurugan, G.; Ganapathy, R.; Maiti, P. K.; Jayaraman, N.; Sood, A. K. *Journal of Chemical Physics* **2006**, *124*.
(45) Lee, H.; Baker, J. R.; Larson, R. G. *Journal of Physical Chemistry B* **2006**, *110*, 4014.
(46) Welch, P.; Muthukumar, M. *Macromolecules* **1998**, *31*, 5892.
(47) Lee, I.; Athey, B. D.; Wetzel, A. W.; Meixner, W.; Baker, J. R. *Macromolecules* **2002**, *35*, 4510.
(48) Terao, T.; Nakayama, T. *Macromolecules* **2004**, *37*, 4686.
(49) Lin, S. T.; Maiti, P. K.; Goddard, W. A. *Journal of Physical Chemistry B* **2005**, *109*, 8663.
(50) Maiti, P. K.; Goddard, W. A. *Journal of Physical Chemistry B* **2006**, *110*, 25628.
(51) Gurtovenko, A. A.; Lyulin, S. V.; Karttunen, M.; Vattulainen, I. *Journal of Chemical Physics* **2006**, *124*, 094904.
(52) Giupponi, G.; Buzza, D. M. A.; Adolf, D. B. *Macromolecules* **2007**, *40*, 5959.
(53) Maiti, P. K.; Bagchi, B. *Journal of Chemical Physics* **2009**, *131*.
(54) Maiti, P. K.; Messina, R. *Macromolecules* **2008**, *41*, 5002.

(55) Maingi, V.; Jain, V.; Bharatam, P. V.; Maiti, P. K. *Journal of Computational Chemistry* **2012**, *33*, 1997.

(56) Kanchi, S.; Suresh, G.; Priyakumar, U. D.; Ayappa, K. G.; Maiti, P. K. *Journal Of Physical Chemistry B* **2015**, *119*, 12990.

(57) Leclaire, J.; Coppel, Y.; Caminade, A. M.; Majoral, J. P. *Journal of the American Chemical Society* **2004**, *126*, 2304.

(58) Cagin, T.; Wang, G. F.; Martin, R.; Breen, N.; Goddard, W. A. *Nanotechnology* **2000**, *11*, 77.

(59) Maiti, P. K.; Li, Y.; Cagin, T.; Goddard, W. A., III. *Journal of Chemical Physics* **2009**, *130*.

(60) Li, Y. Y.; Lin, S. T.; Goddard, W. A. *Journal of the American Chemical Society* **2004**, *126*, 1872.

(61) Lin, S. T.; Jang, S. S.; Cagin, T.; Goddard, W. A. *Journal of Physical Chemistry B* **2004**, *108*, 10041.

(62) Jang, S. S.; Lin, S. T.; Cagin, T.; Molinero, V.; Goddard, W. A. *Journal of Physical Chemistry B* **2005**, *109*, 10154.

(63) Rappe, A. K., Goddard, W. A. III. *J. Phys. Chem* **1991**, *95*, 3358.

(64) Case, D. A.; Pearlman, D. A.; Caldwell, J. W.; Cheatham, T. E.; Wang, J.; Ross, W. S.; Simmerling, C.; Darden, T.; Merz, K. M.; Stanton, R. V.; al., e. AMBER7; 7 ed.; University of California, San Francisco., 1999.

(65) Mayo, S. L.; Olafson, B. D.; Goddard, W. A. *Journal of Physical Chemistry* **1990**, *94*, 8897.

(66) Darden, T., York D., Pedersen L. *J Chem Phys* **1993**, *98*, 10089.

(67) Chen, W. R.; Porcar, L.; Liu, Y.; Butler, P. D.; Magid, L. J. *Macromolecules* **2007**, *40*, 5887.

(68) Bhattacharya, R.; Kanchi, S.; Roobala, C.; Lakshminarayanan, A.; Seeck, O. H.; Maiti, P. K.; Ayappa, K. G.; Jayaraman, N.; Basu, J. K. *Soft Matter* **2014**, *10*, 7577.

(69) Evmenenko, G.; Bauer, B. J.; Kleppinger, R.; Forier, B.; Dehaen, W.; Amis, E. J.; Mischenko, N.; Reynaers, H. *Macromolecular Chemistry and Physics* **2001**, *202*, 891.

(70) Kuklin, A. I.; Ozerin, A. N.; Islamov, A. K.; Muzafarov, A. M.; Gordeliy, V. I.; Rebrov, E. A.; Ignat'eva, G. M.; Tatarinova, E. A.; Mukhamedzyanov, R. I.; Ozerina, L. A.; Sharipov, E. Y. *Journal of Applied Crystallography* **2003**, *36*, 679.

(71) Pavan, G. M.; Barducci, A.; Albertazzi, L.; Parrinello, M. *Soft Matter* **2013**, *9*, 2593.

(72) Zamanakos, G. A Fast and Accurate Analytical Method for the computation of Solvent effects in Molecular simulations, Caltech, 2002.

(73) Vaidehi, N.; Floriano, W. B.; Trabanino, R.; Hall, S. E.; Freddolino, P.; Choi, E. J.; Zamanakos, G.; Goddard, W. A. *Proceedings of the National Academy of Sciences of the United States of America* **2002**, *99*, 12622.

(74) Maiti, P. K.; Pascal, T. A.; Vaidehi, N.; Heo, J.; Goddard, W. A. *Biophysical Journal* **2006**, *90*, 1463.

(75) Maiti, P. K.; Pascal, T. A.; Vaidehi, N.; Goddard, W. A. *NUCLEIC ACIDS RES* **2004**, *32*, 6047.

(76) Jain, V.; Maiti, P. K.; Bharatam, P. V. *Journal Of Chemical Physics* **2016**, *145*, 124902.

(77) Maingi, V.; Kumar, M. V. S.; Maiti, P. K. *Journal Of Physical Chemistry B* **2012**, *116*, 4370.

(78) Lim, J.; Pavan, G. M.; Annunziata, O.; Simanek, E. E. *Journal Of The American Chemical Society* **2012**, *134*, 1942.

(79) Rathgeber, S.; Monkenbusch, M.; Kreitschmann, M.; Urban, V.; Brulet, A. *Journal of Chemical Physics* **2002**, *117*, 4047.

Table 1*: Number of atoms as well as number of primary and tertiary amines for various generations fully atomistic PAMAM dendrimer.*

Generation	Number of Atoms	Number of primary amines	Number of tertiary amines
0	84	4	2
1	228	8	6
2	516	16	14
3	1092	32	30
4	2244	64	62
5	4548	128	126
6	9156	256	254
7	18372	512	510
8	36804	1024	1022
9	73668	2048	2046

Table 2: Radius of gyration (R_g) of various generation PAMAM dendrimers at high and neutral pH. Shown are also the sizes determined from SAXS and SANS experiment.

Generation	R_g (Å) this work			R_g (Å) Experiment	
	High pH	Neutral pH	Low pH	SAXS[79]	SANS
1	7.4	9.4	9.5	7.9	
2	11.5	13.6	13.9	11.8	
3	12.9	17.2	16.8	15.09	
4	16.9	21.7	21.5	18.6	
5	20.3	26.1	27.0	23.07	24.3
6	24.7	32.5	31.9	27.5	
7	30.1	37.57	37.1	32.1	34.4
8	37.83	42.94	43.1	38.58	39.5
9	46.39	51.83	51.68	49.2	

Table 3: Number of inner water molecule as a function of dendrimer generations at various pH. For the criteria used to calculate number of inner waters see the text.

Generation	Number of inner water molecules		
	High pH	Neutral pH	Low pH
2	7	26	20
3	38	72	109
4	97	195	288
5	297	505	778
6	483	1401	2067
7	719	3144	4198
8	719	3144	6633
9	8661	33261	37773

Table 4: Available solvent accessible surface area (SASA) and volume (SAV) as a function of dendrimer generation for various solvent conditions for a probe radius of 1.4 Å.

Generation	High pH		Neutral pH		Low pH	
	SASA ($Å^2$)	SAV ($Å^3$)	SASA ($Å^2$)	SAV ($Å^3$)	SASA ($Å^2$)	SAV ($Å^3$)
2	287.26	2080.17	272.16	4858.9	304.19	5884.04
3	733.28	5245.5	502.39	13011.5	1467.83	12776.1
4	1849.1	8749.1	4140.2	28111.22	6749.2	33336.9
5	4719.2	13614.7	10097.03	51598.2	15899.58	58958.5
6	10418.7	25263.3	30546.09	98940.8	44968.16	108320.97
7	23891	47771.9	66800.3	149782.1	71941.89	151195.9

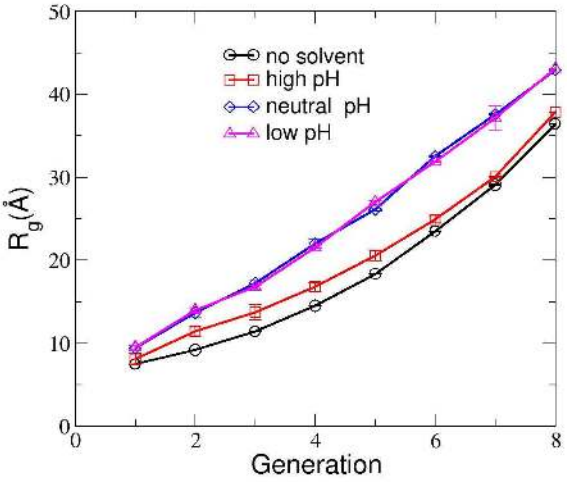

Figure 1: R_g for various generation dendrimers at high pH and neutral pH as a function of dendrimer generations. Lines are guide to the eye only.

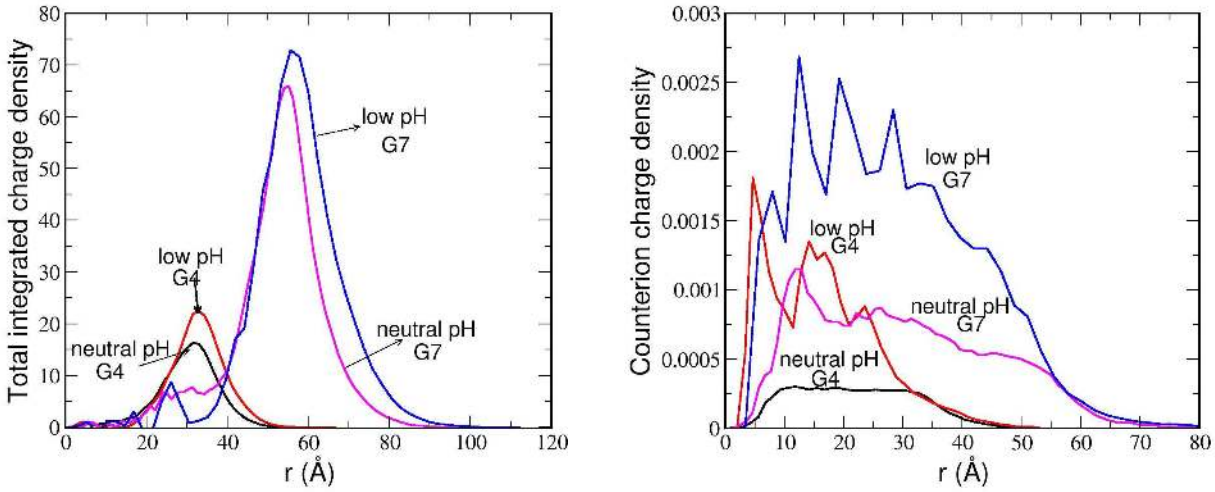

Figure 2: (a) Total integrated charge density for G4 and G7 PAMAM dendrimer at neutral and low pH. Note that the charge neutral regime is larger at low pH compared to neutral pH due to accumulation of larger number of counterions (Cl- ions) in the interior of the dendrimer. (b) Counterion charge density for G4 and G7 PAMAM dendrimer at neutral and low pH. At low pH more number if Cl- ions penetrate in the interior of the dendrimer.

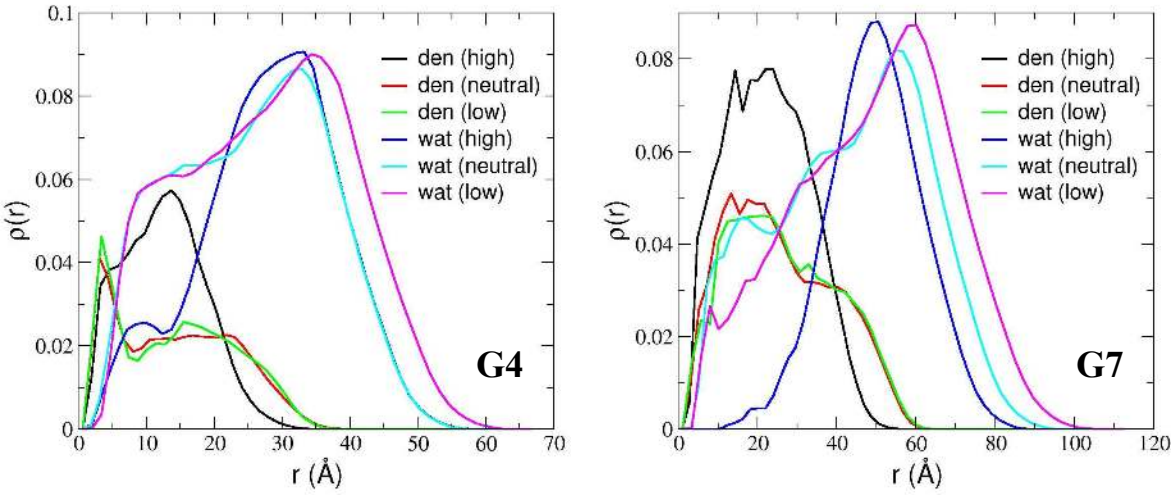

Figure 3: Radial monomer density distribution for (a) G4 and (b) G7 dendrimer at various solvent conditions. We also show the water density distribution to demonstrate the degree of water penetration.

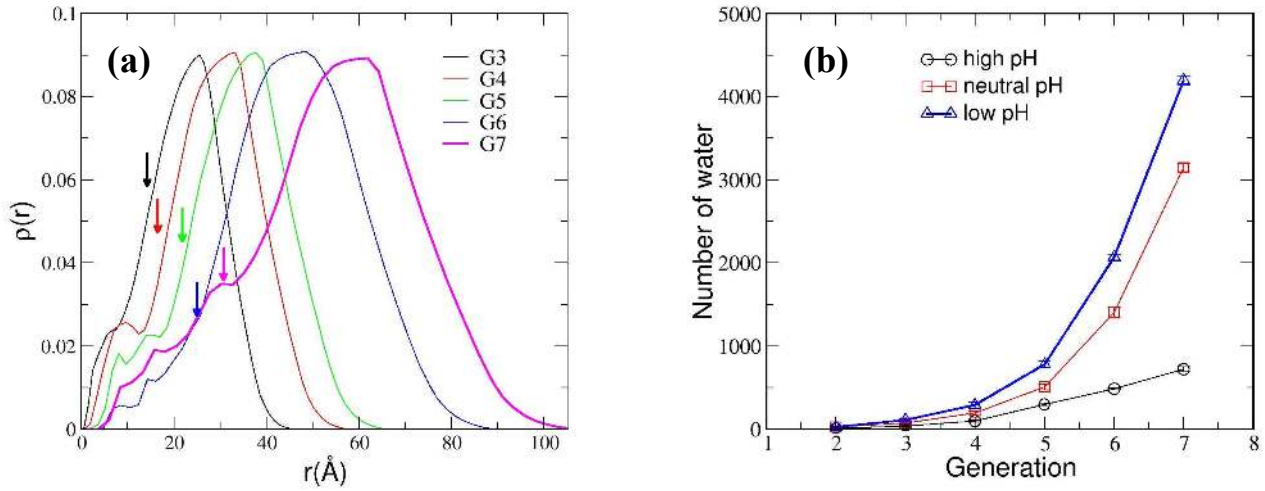

Figure 4: (a) water density profile for various generation PAMAM dendrimer at high pH. The arrow denotes the position corresponding to the radius of gyration (R_g). (b) Number of water as a function generation at various pH.

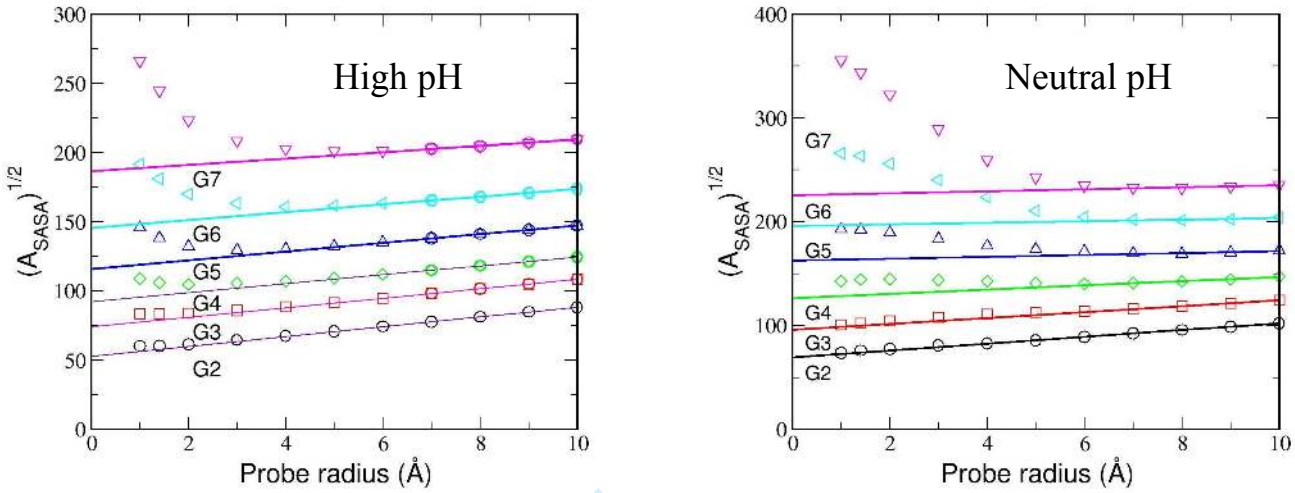

Figure 5: $\sqrt{A_{SAS}}$ *as a function of probe radius for various generations PAMAM dendrimer at (a) high pH and (b) neutral pH . The line fitting larger probe radii extrapolated to zero probe radius provides a measure of the outside area (excluding pores and internal voids) while the difference between the calculated points and this line gives the internal area of the pores and internal voids.*

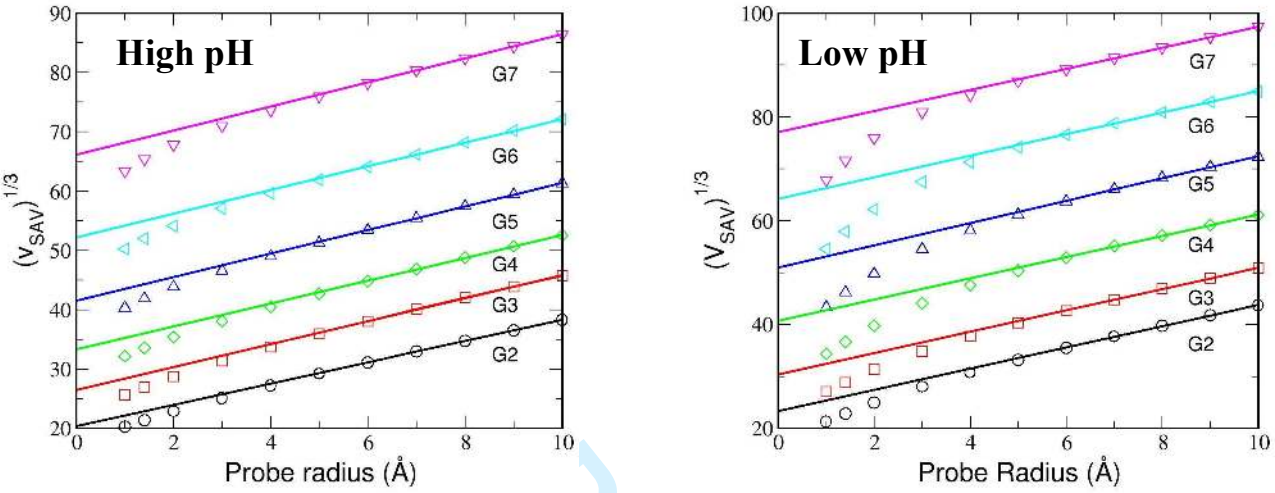

Figure 6: $V_{SAS}^{1/3}$ as a function of probe radius for various generations PAMAM dendrimer. The line fitting larger probe radius extrapolated to zero probe radius provides a measure of the total volume (including pores and internal voids) while the difference between the calculated points and this line gives the internal volume of the pores and internal voids.

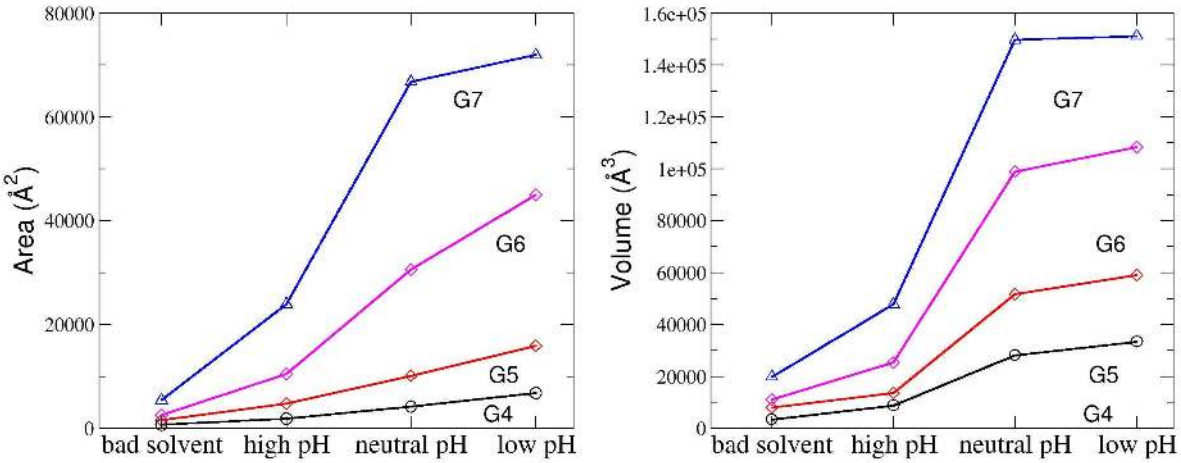

Figure 7: (a) Change in the solvent accessible surface area and (b) Solvent accessible volume for G4-G7 PAMAM dendrimer at various solvent conditions.